Effective low-order models for atmospheric dynamics and time series analysis

Alexander Gluhovsky and Kevin Grady

Citation: Chaos **26**, 023119 (2016); doi: 10.1063/1.4942586
View online: http://dx.doi.org/10.1063/1.4942586
View Table of Contents: http://scitation.aip.org/content/aip/journal/chaos/26/2?ver=pdfcov
Published by the AIP Publishing

Effective low-order models for atmospheric dynamics and time series analysis

Alexander Gluhovsky[1,2,a)] and Kevin Grady[1]
[1]*Department of Earth, Atmospheric, and Planetary Sciences, Purdue University, West Lafayette, Indiana 47907, USA*
[2]*Department of Statistics, Purdue University, West Lafayette, Indiana 47907, USA*

(Received 24 September 2015; accepted 11 February 2016; published online 26 February 2016)

The paper focuses on two interrelated problems: developing physically sound low-order models (LOMs) for atmospheric dynamics and employing them as novel time-series models to overcome deficiencies in current atmospheric time series analysis. The first problem is warranted since arbitrary truncations in the Galerkin method (commonly used to derive LOMs) may result in LOMs that violate fundamental conservation properties of the original equations, causing unphysical behaviors such as unbounded solutions. In contrast, the LOMs we offer (G-models) are energy conserving, and some retain the Hamiltonian structure of the original equations. This work examines LOMs from recent publications to show that all of them that are physically sound can be converted to G-models, while those that cannot lack energy conservation. Further, motivated by recent progress in statistical properties of dynamical systems, we explore G-models for a new role of atmospheric time series models as their data generating mechanisms are well in line with atmospheric dynamics. Currently used time series models, however, do not specifically utilize the physics of the governing equations and involve strong statistical assumptions rarely met in real data. © *2016 AIP Publishing LLC*. [http://dx.doi.org/10.1063/1.4942586]

Two major sources to advance our understanding of atmospheric dynamics are governing equations and field observations. The equations, however, present enormous mathematical challenges, whereas observed records are commonly analyzed via time series models, often involving unrealistic assumptions. Following Kolmogorov described in Ref. 1, Lorenz,[2,3] and Obukhov,[4,5] a popular approach to handle the governing partial differential equations (PDEs) is to approximate them with finite systems of ordinary differential equations (ODEs), called low-order models (LOMs). One such LOM is the celebrated Lorenz model[3] of just three ODEs, but attempts to extend it to larger, more realistic models of atmospheric dynamics have sometimes led to LOMs exhibiting unphysical behaviors. These do not occur in the LOMs we develop (G-models,[6] the simplest one equivalent[7] to the Lorenz model). We show that all recent physically sound LOMs can be converted to G-models, while those lacking such presentation are not energy-conserving. This suggests that G-models may offer a general framework for deriving effective LOMs in atmospheric dynamics. In particular, G-models are proposed here as novel atmospheric time series models, thereby utilizing their probabilistic facet. In contrast to common ones (borrowed from traditional time series analysis and having little to do with the atmosphere per se), G-models are derived from the underlying equations, and so their statistical behavior is in better agreement with reality.

I. INTRODUCTION

Solutions of the governing nonlinear PDEs of atmospheric dynamics are elusive, but their easier to handle approximations, the low-order models (LOMs), reveal basic mechanisms and their interplay through focusing on key elements and retaining only minimal numbers of degrees of freedom. LOMs are commonly derived from the PDEs via the Galerkin method: fluid dynamical fields are expanded into infinite series in time-independent basis functions (commonly Fourier modes), then the series are truncated and substituted into the PDEs yielding a finite system of ODEs (the LOM) for the time evolution of the coefficients in the truncated expansions. Obukhov[4] showed that the simplest nonlinear LOM is a 3-mode (3-ODEs) system equivalent to the Euler gyroscope and suggested systems of coupled Euler gyroscopes for modeling homogeneous flows.[5] Earlier Lorenz[2] had introduced an equivalent LOM as the simplest model of atmospheric dynamics. Pasini and Pelino[1] discuss in a geometric framework the Lorenz[2,3] and Obukhov[4] systems as included in a general class of 3-mode LOMs introduced by Kolmogorov in 1958 at his seminar on dynamical systems.

Both Lorenz and Obukhov insisted that LOMs should retain conservation properties of the original PDEs. Arbitrary truncations in the Galerkin method, however, can lead to models that lack the fundamental physical properties of the original equations, such as energy conservation (here and throughout the paper understood as conservation in the limit of no damping and forcing). The problem was addressed[6,7] by constructing LOMs in the form of coupled 3-mode nonlinear dynamical systems known in mechanics as Volterra gyrostats. The Volterra gyrostat,[8,9]

a)Electronic mail: aglu@purdue.edu.

$$\begin{aligned} I_1\dot{\omega}_1 &= (I_2 - I_3)\omega_2\omega_3 + h_2\omega_3 - h_3\omega_2, \\ I_2\dot{\omega}_2 &= (I_3 - I_1)\omega_3\omega_1 + h_3\omega_1 - h_1\omega_3, \\ I_3\dot{\omega}_3 &= (I_1 - I_2)\omega_1\omega_2 + h_1\omega_2 - h_2\omega_1, \end{aligned} \tag{1}$$

is a classical system, which admits various mechanical and fluid dynamical interpretations (e.g., Ref. 10 and 11). It can be thought of as a rigid body containing an axisymmetric rotor that rotates with a constant angular velocity about an axis fixed in the carrier. In this interpretation, I_i are the principal moments of inertia of the gyrostat, $\boldsymbol{\omega}$ is the angular velocity of the carrier body, and $\boldsymbol{h}$ is the fixed angular momentum caused by the relative motion of the rotor (the gyrostatic motion). In Eqs. (1) and everywhere below, the overdot means differentiation with respect to time. Eqs. (1) have two quadratic invariants, the kinetic energy, $E = \sum I_i\omega_i^2/2$, and the square of the angular momentum, $C = \sum (I_i\omega_i + h_i)^2$. Note that unlike linear friction terms, linear terms in Eqs. (1) (*linear gyrostatic terms*) do not affect the conservation of energy nor the conservation of phase space volume.

We call two LOMs equivalent if one can be obtained from the other by a linear change of variables. For example, it is often convenient to write Eqs. (1) in terms of variables $X_i = \sqrt{I_i}\omega_i$ (then the kinetic energy becomes $E = \sum X_i^2/2$)

$$\begin{aligned} \dot{X}_1 &= pX_2X_3 + bX_3 - cX_2, \\ \dot{X}_2 &= qX_3X_1 + cX_1 - aX_3, \\ \dot{X}_3 &= rX_1X_2 + aX_2 - bX_1, \end{aligned} \tag{2}$$

where $p = J(I_2 - I_3), q = J(I_3 - I_1), \quad r = J(I_1 - I_2), \; p + q + r = 0; a = Jh_1\sqrt{I_1}, b = Jh_2\sqrt{I_2}, c = Jh_3\sqrt{I_3}$.[10] More importantly, the simplest Volterra gyrostat ($I_1 = I_2$ and $h_2 = h_3 = 0$ in Eqs. (1), or $r = b = c = 0$ in Eqs. (2)) in a forced regime (i.e., with added constant forcing and linear friction), which can be written[6] as

$$\left.\begin{array}{l|l|l} \dot{x}_1 = & -x_2x_3 & -\alpha_1x_1 + F, \\ \dot{x}_2 = & x_3x_1 - x_3 & -\alpha_2x_2, \\ \dot{x}_3 = & x_2 & -\alpha_3x_3, \end{array}\right. \tag{3}$$

was proved[7] to be equivalent to the celebrated Lorenz (or Lorenz-63) model[3] of two-dimensional Rayleigh-Bénard convection (2D RBC),

$$\dot{x} = \sigma(y - x), \quad \dot{y} = -xz + rx - y, \quad \dot{z} = xy - bz, \tag{4}$$

(for this reason we call (3) the *Lorenz gyrostat*). In Eqs. (3) and others below, separate Volterra gyrostats are shown within vertical bars, variables are denoted by x_i, friction coefficients by α_i, forces by F.

It was found[12,13] that effective LOMs for atmospheric circulations and turbulence could be developed as systems of *coupled* gyrostats (2). For example, the following 5-mode system:[14]

$$\left.\begin{array}{l|l|l|l} \dot{x}_1 = & -x_2x_3 & -x_4x_5 & -\alpha_1x_1 + F, \\ \dot{x}_2 = & x_3x_1 - x_3 & & -\alpha_2x_2, \\ \dot{x}_3 = & x_2 & & -\alpha_3x_3, \\ \dot{x}_4 = & & x_5x_1 - x_5 & -\alpha_4x_4, \\ \dot{x}_5 = & & x_4 & -\alpha_5x_5, \end{array}\right. \tag{5}$$

offers an analog of the Lorenz model (4) for *3D* RBC, where two Lorenz gyrostats describe the dynamics in two perpendicular planes.

Also, similar to the Arnold's definition of the *n*-dimensional rigid body,[15] the *n-dimensional gyrostat* was introduced[6,7] as the *n*-dimensional analog of the Volterra equations (1), with Eqs. (1) recovered by setting $n = 3$. This construction permits another look at system (5) as a 4-dimensional gyrostat (in a forced regime),[6] and the 6-mode extension of the Lorenz model (4), recently suggested[16] as a more appropriate minimal model of 2D RBC than (4), proves equivalent to another 4-dimensional gyrostat.[17]

We call all gyrostat-based LOMs (Volterra gyrostats, coupled gyrostats, *n*-dimensional gyrostats) *gyrostatic low-order models*,[6] or for brevity *G-models*. G-models conserve energy in the dissipationless limit, and their modular nature enables the creation of new physically sound LOMs through the addition or removal of gyrostats in existing models.

The latter, for example, proves instrumental in developing Hamiltonian LOMs,[6] which is important since the conservative part of various atmospheric models (the primitive equations, shallow water equations, quasi-geostrophic equations) is Hamiltonian (e.g., Ref. 18). A finite-dimensional Hamiltonian dynamical system may be written[18,19] as

$$\dot{x}_i = J_{ij}\frac{\partial H}{\partial x_j}, \tag{6}$$

where H is the Hamiltonian function and J is an antisymmetric matrix ($J_{ij} - J_{ji}$) satisfying the Jacobi conditions,

$$J_{il}\frac{\partial J_{jk}}{\partial x_l} + J_{jl}\frac{\partial J_{ki}}{\partial x_l} + J_{kl}\frac{\partial J_{ij}}{\partial x_l} = 0, \tag{7}$$

(repeated indices imply summation). Now, all G-models possess a constant of motion (representing some form of energy)

$$H = \sum x_i^2/2, \tag{8}$$

which is a good candidate for the Hamiltonian function, and they all are readily presented in form (6) with an easily determined antisymmetric matrix J, for which it is pretty straightforward to check the Jacobi conditions (7).[6] For example,[6] G-model (2) has the Hamiltonian form (6) with $H = (x_1^2 + x_2^2 + x_3^2)/2$ and antisymmetric matrix

$$J = \begin{pmatrix} 0 & -c & px_2 + b \\ c & 0 & qx_1 - a \\ -(px_2 + b) & -(qx_1 - a) & 0 \end{pmatrix}.$$

Similar to the Volterra gyrostat (1), other G-models may have constants of motion in addition to (8) (e.g., Refs. 6, 10, 17, and 20).

In this paper, we explore the LOMs of 2D RBC (the 3D case will be addressed separately). Of fundamental importance in nonlinear dynamics, where it is the most carefully studied example of nonlinear systems exhibiting self-organization and transition to chaos, RBC (e.g., Ref. 21) promotes understanding of many real-world fluid flows by providing the principal mechanism of mesoscale shallow convection in the atmosphere[22] and

being also important for studies of flows in oceanic flows, in the liquid core of the Earth, and in astrophysics.

We have found that all physically sound LOMs of 2D RBC that have appeared in recent publications are equivalent to G-models, while the LOMs that cannot be converted to gyrostats exhibit violations of energy conservation (Sec. II). This suggests that G-models may offer a general framework for developing effective LOMs for studies in atmospheric dynamics (some have already been variously employed in this area, see Refs. 6 and 17 and references therein).

A new promising application of G-models (introduced in Sec. III) is motivated by current problems with handling atmospheric data on one hand and by recent progress in statistical properties of dynamical systems on the other. It has been proved, in particular, that Lorenz model (4) flow possesses a physical ergodic invariant probability measure[23] and satisfies the central limit theorem,[24,25] i.e., series of observations on this model may exhibit statistics of sequences of random variables. In Sec. III, G-models are explored for the new role of atmospheric time series models, thus infusing more physics in atmospheric time series analysis.

A summary of our results and further discussion are presented in Sec. IV.

II. PHYSICALLY SOUND LOW-ORDER MODELS OF 2D RAYLEIGH-BÉNARD CONVECTION

A. Equations and Galerkin expansions

The 2D RBC (a buoyancy-driven flow between two horizontal, isothermal surfaces, with the lower one at higher temperature) is commonly described by the equations in the Boussinesq approximation (e.g., Refs. 26–28)

$$\frac{D\nabla^2\psi}{Dt}=\frac{\partial\theta}{\partial x}+\nu\nabla^4\psi,\quad \frac{D\theta}{Dt}=\frac{\partial\psi}{\partial x}+\kappa\nabla^2\theta, \tag{9}$$

where ψ is the stream function so that $v=(-\partial_z\psi,\partial_x\psi)$ is the velocity field, $D/Dt=\partial/\partial t+v\cdot\nabla$ is the so-called material derivative, all quantities are dimensionless (as in Ref. 27), x is the horizontal coordinate, z is the vertical one, θ is the deviation of the temperature from a linear conduction profile, ν is the kinematic viscosity, and κ is the thermal conductivity.

The so-called "free" boundary conditions are commonly imposed at both the top and the bottom of the fluid, mostly as[26]

$$\psi=\nabla^2\psi=\theta=0,\quad z=0,\pi. \tag{10}$$

Via expanding ψ and θ into infinite series in time-independent basis functions satisfying boundary conditions, selecting a finite number of the terms in the expansions, and substituting the latter in Eqs. (9), numerous LOMs for 2D RBC have been obtained, some of them are energy-conserving, whereas others are not.

Widely used are the following Galerkin expansions:[3,16,26]

$$\psi(t,x,z)=\sum_{m=0}^{\infty}\sum_{n=1}^{\infty}(\psi_{m,n}(t)\sin amx+\phi_{m,n}(t)\cos amx)\sin nz,$$
$$\theta(t,x,z)=\sum_{m=0}^{\infty}\sum_{n=1}^{\infty}(\theta_{m,n}(t)\cos amx+\vartheta_{m,n}(t)\sin amx)\sin nz. \tag{11}$$

Treve and Manley[27] have provided necessary and sufficient conditions for a LOM of 2D RBC to be energy-conserving. Their l-order Gelerkin expansion,

$$\psi^{(l)}(t,x,z)=\sum_{E}\psi_{m,n}(t)\sin amx\sin nz,$$
$$\theta^{(l)}(t,x,z)=\sum_{E}\theta_{m,n}\sin amx\sin nz+\sum_{n=1}^{\bar n}\theta_{m,n}(t)\sin nz, \tag{12}$$

is defined by the first l terms of the ascending sequence

$$\rho_{1,1}=\rho_{m_1,n_1}\le\rho_{m_2,n_2}\le\cdots\rho_{m_l,n_l} \tag{13}$$

of the eigenvalues $\rho_{m,n}=a^2m^2+n^2$ of the linear problem that determines the basis functions for $\psi(t,\ x,\ z)$, and the sums in Eqs. (12) are over the set E of pairs $(m_i,\ n_i)$ from Eq. (13), $m_i,n_i>0$, $\bar n=\max_{1\le i\le l}n_i$.

Boundary conditions (10) allow for the derivation of the most general LOMs using the full Galerkin expansions of ψ and θ. Additional periodic horizontal boundary conditions[27]

$$\partial_z\psi=\partial_x\theta=0,\quad x=0,\pi/a, \tag{14}$$

where a is the inverse aspect ratio, exclude some modes from the expansions of ψ and θ, which permits only a certain class of LOM, narrower than that allowed when using the boundary conditions (10) only. The less explicit horizontal boundary conditions that the fluid is periodic in the horizontal (i.e., $(x,\ z)\in[0,\ 2\pi/a]\times[0,\ \pi]$) are sometimes employed, e.g., to allow for vertical shear.[28]

B. Results

Tables I and II sum up our results on important LOMs to the effect that all those energy-conserving among them are presentable as G-models.

The upper half of Table I lists four LOMs derived following the mode selection procedure suggested in Ref. 27. All such LOMs may be converted to G-models.[33] The first-order approximation LOM (based on $\rho_{1,1}$ in Eq. (13) and therefore on three modes: $\psi_{1,1}$, $\theta_{1,1}$, and $\theta_{0,2}$) is equivalent to the Lorenz model (4) and gyrostat (3). The next one is the LOM[12] based (when $a<1$) on $\rho_{1,1}$, $\rho_{2,1}$ and, accordingly, on modes $\psi_{1,1}$, $\theta_{1,1}$, $\theta_{0,2}$, $\psi_{2,1}$, $\theta_{2,1}$

$$\begin{array}{l|l|l|l}\dot x_1= & -x_2x_3 & -dx_4x_5 & -\alpha_1x_1+F,\\ \dot x_2= & x_3x_1-x_3 & & -\alpha_2x_2,\\ \dot x_3= & x_2 & & -\alpha_3x_3,\\ \dot x_4= & & dx_5x_1-dx_5 & -\alpha_4x_4,\\ \dot x_5= & & dx_4 & -\alpha_5x_5,\end{array} \tag{15}$$

where $d=\sqrt{\rho_{1,1}/\rho_{2,1}}$. Both these G-models are Hamiltonian with $H=\sum x_i^2/2$, while the next two are not (though they might be that with a different Hamiltonian function, see an example below).

Interestingly, the conservative parts of LOMs (5) and (15) look similar (recall, however, that friction coefficients α_i and forces F are different). Moreover, a LOM equivalent to

TABLE I. LOMs with various number of modes (N) kept in Galerkin expansions (12). Other columns specify whether or not they are energy-conserving (EC), gyrostatic (G), and Hamiltonian (H) with Hamiltonian function (8).

Modes in Galerkin expansions	N	EC	G	H
$\psi_{1,1}, \theta_{1,1}, \theta_{0,2}$ (Ref. 3)	3	Yes	Yes	Yes
$\psi_{1,1}, \theta_{1,1}, \psi_{2,1}, \theta_{2,1}, \theta_{0,2}$ (Ref. 12)	5	Yes	Yes	Yes
$\psi_{1,1}, \theta_{1,1}, \psi_{2,1}, \theta_{2,1}, \psi_{1,2}, \theta_{1,2}, \theta_{0,2}, \theta_{0,4}$ (Ref. 29)	8	Yes	Yes	No
$\psi_{1,1}, \theta_{1,1}, \psi_{2,1}, \theta_{2,1}, \psi_{3,1}, \theta_{3,1}, \psi_{1,2}, \theta_{1,2}, \theta_{0,2}, \theta_{0,4}$ (this study)	10	Yes	Yes	No
$\psi_{1,1}, \theta_{1,1}, \theta_{0,2}, \theta_{0,4}, \theta_{1,3}$ (Ref. 30)	5	Yes	Yes	No
$\psi_{1,1}, \theta_{1,1}, \theta_{0,2}, \theta_{0,4}, \theta_{1,3}, \psi_{1,3}$ (Ref. 31)	6	No	No	No
$\psi_{1,1}, \theta_{1,1}, \theta_{0,2}, \theta_{0,4}, \theta_{1,3}, \psi_{1,3}, \theta_{0,6}$ (this study)	7	Yes	Yes	No
$\psi_{1,1}, \theta_{1,1}, \psi_{1,3}, \theta_{1,3}, \psi_{2,2}, \theta_{2,2}, \psi_{3,1}, \theta_{3,1}, \psi_{3,3}, \theta_{3,3}, \psi_{2,4}, \theta_{2,4}, \theta_{0,2}, \theta_{0,4}$ (Ref. 32)	14	No	No	No

(5) was later suggested[34] (using expansion (11)) as an improvement on the Lorenz model (4).

The four LOMs in the bottom half of Table I exemplify the case when still using expansions expansions (12), the mode selection in Ref. 27 is violated. The resulting LOM then may still be energy-conserving, as the LOM considered in Ref. 30 (based on modes $\psi_{1,1}$, $\theta_{1,1}$, $\theta_{0,2}$, $\theta_{1,3}$, $\theta_{0,4}$, with $\theta_{0,6}$ required in Ref. 27 missing) thus permitting, as we have found, a G-model form

$$\begin{vmatrix} \dot{x}_1 = \\ \dot{x}_2 = \\ \dot{x}_3 = \\ \dot{x}_4 = \\ \dot{x}_5 = \end{vmatrix} \begin{vmatrix} -x_2x_3 \\ x_3x_1 - x_3 \\ x_2 \\ \\ \end{vmatrix} \begin{vmatrix} +x_3x_4 \\ \\ \\ -x_1x_3 \\ \end{vmatrix} \begin{vmatrix} \\ \\ \\ +2x_3x_5 \\ -2x_3x_4 \end{vmatrix} \begin{vmatrix} -\alpha_1x_1 + F, \\ -\alpha_2x_2, \\ -\alpha_3x_3, \\ -\alpha_4x_4, \\ -\alpha_5x_5, \end{vmatrix} \tag{16}$$

Or the resulting LOM may prove to be not energy-conserving (and thus cannot be converted to a G-model), such as the system in Ref. 31 based on modes $\psi_{1,1}$, $\theta_{1,1}$, $\theta_{0,2}$, $\psi_{1,3}$, $\theta_{1,3}$, $\theta_{0,4}$ (where again $\theta_{0,6}$ is missing) and a well-known 14-mode extension[32] of the Lorenz model (4). Then adding a few modes in Galerkin expansions may produce energy-conserving LOMs (having accordingly a G-model form); for example, in the case of the 6-mode model in Ref. 31, adding the $\theta_{0,6}$ mode results in a 7-mode G-model in Table I.

Table II lists LOMs derived from Galerkin expansions in Ref. 26. Although the 3-mode truncation based on $\psi_{1,1}$, $\theta_{1,1}$, $\theta_{0,2}$ again produces the Lorenz model (4) and the next four LOMs are G-models, other truncations of those expansions pursued in a number of studies have not necessarily resulted in energy-conserving LOMs. In Table II, the latter is exemplified by the famous 6-mode Howard-Krishnamurti model[35] of convection with shear that, however, proved lacking the energy and total vorticity conservation. These deficiencies have been remedied by adding a term to a Galerkin temperature expansion[28] and another term to the stream function expansion,[36] which has resulted in a 8-mode G-model composed of six gyrostats.[20] By deleting three of these gyrostats, a new 6-mode system was obtained[20] still describing the desired effect while respecting the conservation laws.

TABLE II. LOMs with various number of modes (N) kept in Galerkin expansions (11). Other columns specify whether or not they are energy-conserving (EC), gyrostatic (G), and Hamiltonian (H) with Hamiltonian function (8).

Modes in Galerkin expansions	N	EC	G	H
$\psi_{1,1}, \theta_{1,1}, \theta_{0,2}$ (Ref. 3)	3	Yes	Yes	Yes
$\psi_{1,1}, \theta_{1,1}, \phi_{1,1}, \vartheta_{1,1}, \theta_{0,2}$ (Ref. 34)	5	Yes	Yes	Yes
$\psi_{1,1}, \theta_{1,1}, \phi_{1,1}, \vartheta_{1,1}, \theta_{0,2}$ (Ref. 16)	5	Yes	Yes	No
$\psi_{1,1}, \theta_{1,1}, \phi_{1,1}, \vartheta_{1,1}, \theta_{1,3}, \vartheta_{1,3}, \theta_{0,2}, \theta_{0,4}$ (this study)	8	Yes	Yes	No
$\psi_{1,1}, \theta_{1,1}, \psi_{0,1}, \phi_{1,2}, \vartheta_{1,2}, \theta_{0,2}$ (Ref. 35)	6	No	No	No
$\psi_{1,1}, \theta_{1,1}, \psi_{0,1}, \phi_{1,2}, \vartheta_{1,2}, \theta_{0,2}, \psi_{0,3}, \theta_{0,4}$ (Ref. 20)	8	Yes	Yes	No
$\psi_{1,1}, \theta_{1,1}, \psi_{0,1}, \phi_{1,2}, \theta_{0,2}, \psi_{0,3}$ (Ref. 20)	6	Yes	Yes	No

Note that an important Hamiltonian LOM by Bihlo and Staufer,[16] in gyrostatic form,[17]

$$\begin{vmatrix} \dot{x}_1 = \\ \dot{x}_2 = \\ \dot{x}_3 = \\ \dot{x}_4 = \\ \dot{x}_5 = \end{vmatrix} \begin{vmatrix} -x_2x_3 \\ x_3x_1 - c_1x_3 \\ c_1x_2 \\ \\ \end{vmatrix} \begin{vmatrix} -x_4x_5 \\ \\ \\ x_5x_1 - c_1x_5 \\ c_1x_4 \end{vmatrix} \begin{vmatrix} \\ -c_2x_4 \\ \\ +c_2x_2 \\ \end{vmatrix} \begin{vmatrix} \\ \\ -c_3x_5 \\ \\ +c_3x_3 \end{vmatrix} \tag{17}$$

has a Hamiltonian function different from (8) (and therefore marked "No" in the column of Table II indicating Hamiltonian systems with $H = \sum x_i^2/2$), but it becomes a Hamiltonian system with Hamiltonian function (8) simply by deleting one gyrostat (with coefficients c_3). The latter also illustrates how G-models enable the creation of new physically sound LOMs via addition or removal of gyrostats in existing models.

In summary, there is no way to determine *a priori* whether a LOM based on a particular mode selection will be energy-conserving, unless the procedure in Ref. 27 was followed. In contrast, G-models obtained via whatever Galerkin truncations are always energy-conserving and sometimes easy to modify to obtain smaller G-models (including Hamiltonian ones) describing the effect of interest.

Although we chose to focus on RBC in this paper, gyrostatic models have been developed for a range of other applications in atmospheric dynamics. Among these are other convection problems (e.g., Refs. 6, 17, and 20), the barotropic, quasigeostrophic potential vorticity equation for a beta-plate atmosphere with topography,[20] and shell models for 2D and 3D turbulence,[10,13] where individual Volterra gyrostats are used as building blocks to construct the energy-conserving part of the LOM.

Section III discusses a new application of G-models that capitalizes on their probabilistic facet.

III. NOVEL ATMOSPHERIC TIME SERIES MODELS

A. Problems in current atmospheric time series analysis

Consider, as a typical example, an aircraft record of the vertical velocity of wind in a convective boundary layer taken at 50 m above Lake Michigan during an outbreak of a polar air mass over the Great Lakes region.[37] The sample mean, variance, skewness, and kurtosis computed from its nearly seven-minute stationary segment (shown in Fig. 1) are −0.04, 1.06, 0.83, and 4.10, respectively.

The elevated skewness and kurtosis (from values specific for a normal distribution, 0 and 3) are attributed to the occurrence of coherent structures in turbulent flows,[39] but sample characteristics are just point estimates of the true values of the parameters, and therefore, confidence intervals (CIs) are necessary to learn how far one can trust such numbers. Construction of CIs for parameters of the unknown distribution of a stationary time series from observed records is central to obtaining reliable statistical inference from atmospheric records of limited length, yet difficult in practice due to general problems in atmospheric time series analysis.

A CI traps the unknown parameter with a specified *coverage probability* (say, 0.90). CIs are determined by the data generating mechanism (DGM) and depend on the sample size. For example, a 0.90 (or 90%) CI for the mean of AR(1) (first order autoregressive process widely used in atmospheric studies as a default model for correlated series)

$$Y_t = \phi Y_{t-1} + \epsilon_t \tag{18}$$

obtained from a record of length n with sample mean $\bar{Y}$ is approximately $\bar{Y} \pm 1.645\sigma/\sqrt{n}(1-\phi)$. In Eq. (18), $0 < \phi < 1$ and ϵ_t is a white noise process with mean 0 and variance σ^2.

When the DGM is known, CIs can be found analytically (as in the above example, where the DGM is given by the linear model (18)) or, when analytical results are unavailable, computed from numerous records of length n generated by the *known* (even nonlinear) model. In practice, however, the DGM is *unknown*, and so CIs are commonly computed from linear models *fitted* to the data, thereby often resulting in erroneous CIs, particularly when the real DGM is nonlinear,[40] which is typical for atmospheric time series (generated by the inherently nonlinear system). Besides, CIs for the skewness cannot be based on linear models (implying zero skewness), while finding an appropriate (nonlinear) model among conventional time series models is problematic, as their DGMs are inherently different from the original one.

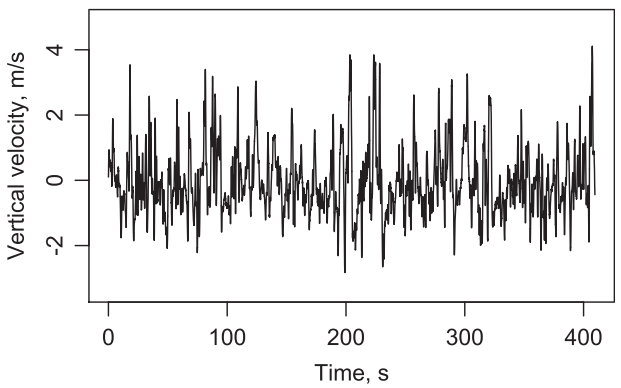

FIG. 1. Record of 20-Hz aircraft vertical velocity measurements over Lake Michigan. Adapted with permission from Gluhovsky, Nonlinear Processes Geophys. **18**, 537 (2011). Copyright 2011 Copernicus Publications. The data are available at http://weather.eaps.purdue.edu/w1.txt.

Models can be avoided by using the bootstrap[41] or other computer-intensive statistical methods such as subsampling,[42] where the above numerous records are replaced by resamples/subsamples obtained from the single record at hand. Atmospheric records, however, are typically too short to satisfy the underlying asymptotic conditions, and so in practice *approximating models* (those sharing statistical properties with the series under study) are used to assess the actual coverage and to adjust the subsampling CIs accordingly.

For a subsampling treatment of the series in Fig. 1, [38] the following approximating model[43] was used (referred below to as model A):

$$X_t = Y_t + a(Y_t^2 - 1), \tag{19}$$

where Y_t is an AR(1) process in Eq. (18) with $\sigma_\epsilon^2 = 1 - \phi^2$ (so that $\sigma_Y^2 = 1$). The reason behind choosing model (19) was that at $a = 0.145$, the first four moments of X_t (0, 1.04, 0.84, 3.95, respectively) were close to the corresponding sample characteristics of the series in Fig. 1 (−0.04, 1.06, 0.83, and 4.10), while setting $\phi = 0.83$ served to fairly imitate its dependence structure as characterized by autocorrelation functions. One could then presume that the model is adequate for fixing subsampling CIs, but there is no guarantee that other statistical properties of the data and the model do not differ to considerably affect the intended applications.

Again, the efficacy of a CI in both cases depends on the record length and on how well the DGM of the model approximates the true one. The former is given, but G-models can improve the latter.

B. A simple G-model for the example data set

As an alternative to model A, Lorenz model (4) (or its equivalent, G-model (3)) looks like a natural choice, since (a) it has well-defined statistical properties mentioned in Section I, and (b) the basic mechanism responsible for producing the series in Fig. 1 is RBC. But the model has proved disappointing, since the skewness and kurtosis calculated from its long records were $S = 0$ and $K = 2.3$, both far off the sample characteristics of the observed series ($S = 0.83$, $K = 4.1$), with the respective subsampling CIs (0.56, 1.1) and (3.7, 4.5).

Consider, however, that in addition to RBC as its principal mechanism, the dynamics over Lake Michigan involves a host of others, such as large-scale vertical motion, cloud top entrainment instability, latent heat release, and gravity waves.[22]

One more feature of G-models (of particular importance for this study) is that mechanisms peculiar to atmospheric

dynamics (e.g., stratification, rotation, topography, shear, magnetohydrodynamic effects) bring about linear gyrostatic terms in these models. For example, the Charney-DeVore model,[44] which has served for a long time as a paradigm of the atmospheric circulation in midlatitudes, involves two such mechanisms, topography and rotation. Accordingly, its G-model version[20] contains gyrostats, exemplified by the following two:

$$\begin{vmatrix} \dot{x}_1 = & b_1 x_3 \\ \dot{x}_2 = & q_1 x_3 x_1 - a_1 x_3 \\ \dot{x}_3 = & -q_1 x_1 x_2 + a_1 x_2 - b_1 x_1 \end{vmatrix} \tag{20}$$

$$\begin{vmatrix} \dot{x}_2 = & p_2 x_4 x_6 \\ \dot{x}_4 = & q_2 x_6 x_2 + b_2 x_6 \\ \dot{x}_6 = & r_2 x_2 x_4 - b_2 x_4 \end{vmatrix} \tag{21}$$

that have two kinds of linear gyrostatic terms: those with coefficients a_i are due to topography and those with b_i are caused by rotation. Note also that both gyrostats differ from the Lorenz gyrostat (3), namely, there are *two* pairs of linear gyrostatic terms in gyrostat (20) and *three* nonlinear terms in gyrostat (21).

These additional mechanisms would have resulted in new linear gyrostatic terms in the G-model (as explained in the end of Section II) had we attempted to derive it rigorously from the governing equations. For now, just one pair of linear gyrostatic terms as representing all such mechanisms was added in Eqs.(3) (those with coefficient c in Eqs. (22) below), leading to a new G-model (model B)

$$\begin{vmatrix} \dot{x}_1 = & -x_2 x_3 + c x_3 & | & -\alpha_1 x_1 + F, \\ \dot{x}_2 = & x_3 x_1 - x_3 & | & -\alpha_2 x_2, \\ \dot{x}_3 = & x_2 - c x_1 & | & -\alpha_3 x_3, \end{vmatrix} \tag{22}$$

In a dramatic improvement, the skewness and kurtosis in model B at $c = 0.35$ proved close to those of the observed series and of model A (see Table III; the results are analytical for model A[38] and obtained from very long records for model B). The same is attained for the three autocorrelation functions (by tweaking parameter ϕ in Eqs. (18) and sampling rates in series generated by Eqs. (22)).

Thus the basic statistical properties of the two models are similar, but model B has an important advantage in that even this very simple G-model shares some fundamental physics with the original system. This helps (a) to better align statistical properties of series generated by the model with those of observed series beyond first moments and autocorrelation functions, (b) to avoid a difficult task of selecting nonlinear time series models solely from statistical characteristics estimated with questionable accuracy, and (c) to run meaningful Monte Carlo simulations, particularly when estimators are more sensitive to properties of the DGM.

TABLE III. Skewness and kurtosis of the observed and modeled time series.

	Skewness	Kurtosis
Observed series (Fig. 1)	0.83	4.1
Model A (Eqs. (19))	0.84	3.9
Model B (Eqs. (22))	0.81	4.2

C. Further steps

In general, to construct a G-model for an observed series, one should start with appropriate governing equations, decide on the "size" of the model, then derive its initial version from these equations,[6,16,17,45] and finally tweak thus obtained model (add other relevant processes, obtain a model in a Hamiltonian form,[6] adjust parameters) to make statistical characteristics of the model closer to those of the observed series. This is how model B was obtained by tweaking Lorenz model (4) for *2D* RBC. Had model B proved inadequate for an intended use, one could consider a G-model for *3D* RBC instead (as the real flow is 3D), such as models (5) or an 8-mode one in Ref. 14.

Yet larger G-models should be even more useful, since they provide increasingly better approximations to the original system. This is because the dynamics generated by fundamental mathematical models of fluid flows are in a sense "asymptotically finite-dimensional" (see the review Ref. 46). Moreover, when in addition to buoyancy, other mechanisms contributing to atmospheric boundary layer dynamics are added, the resulting G-models become more and more realistic, which should favorably reflect in their statistical behavior and feasibility for atmospheric time series analysis.

Among G-models useful in other areas of atmospheric dynamics, which can also be extended to considerable size if needed, are shell models of turbulence,[10,13] models of a barotropic atmosphere with topography and of the thermal convection with shear,[20] and Hamiltonian LOMs.[6]

IV. CONCLUDING REMARKS

Stripped of many attributes of the original equations (one conspicuous difference is the very low number of modes kept in LOMs, 3–14 in those considered here), LOMs should still retain the fundamental characteristics of the equations (conservation properties and the degree of nonlinearity) to fulfill their interpretive role. And LOMs remain widely employed even with ever-increasing computer power since apart from their traditional uses, as noted by Smith,[47] "Although it is unreasonable to expect solutions to low-dimensional problems to generalize to a million dimensional spaces, so too it is unlikely that problems identified in the simplified models will vanish in operational models".

Finite-mode Hamiltonian approximations for 2D hydrodynamics with a major advantage that each model preserves a maximal number of Casimirs were developed by Zeitlin; such modeling, however, only works for flows on the 2D torus and 2D sphere, and cannot be extended for 3D hydrodynamics.[48–50]

There is extensive work on the Nambu formulation (a generalization of the Hamiltonian one) of fluid dynamics (e.g., Refs. 51–55), in particular on finite models of RBC.[16,56,57] Here, we only mention two G-models that are Nambu systems: the Volterra gyrostat[16] and the 4-

dimensional gyrostat[17] equivalent to the 6-mode LOM suggested by Bihlo and Stoffer[16] as an improvement on the Lorenz-63 model.

In contrast to these and other approaches, which may leave out some useful energy-conserving LOMs, G-models (a) permit one to easily find out if a selection of modes results in an energy-conserving LOM, (b) offer a way to possibly modify the resulting LOM to a Hamiltonian one, and (c) provide a form common to all known physically sound LOMs, offering a general framework for developing efficient LOMs for atmospheric dynamics.

Of particular importance is the example discussed in Sec. III. Various problems in atmospheric time series analysis are currently handled via fitting traditional time series models to the data at hand, but finding among them those adequate for atmospheric data is challenging due to inherently nonlinear DGMs and prohibitively short observed records. The latter, in fact, are so short sometimes that it is difficult to even decide on which of several *types* of models is more appropriate.[58] Purely statistical approaches are well justified in areas, where data only are available, but an important advantage of atmospheric dynamics is that in addition to often problematic data, a considerable part of our knowledge is provided by the governing equations. Current time series models, however, do not specifically utilize the physics the equations contain and often involve unrealistic assumptions.

This paper suggests incorporating the underlying equations in the development of time series models in the form of the G-models, which are derived from these equations and, while being much simpler, inherit their fundamental properties. Unlike large numerical models, G-models can be used to generate numerous records required, among other things, in Monte Carlo testing as, for example, the Lorenz-96 model in Ref. 59.

Besides the mentioned above advancements in resampling methodologies (increasingly employed in atmospheric data analyses, e.g., Ref. 60), G-models may be especially helpful in atmospheric applications of the extreme value theory, where problems with commonly used time series analysis models and methods are exacerbated.[61] For example, coherent structures indicated in turbulent flows by elevated skewness and kurtosis[39] may provide the underlying physical mechanism that leads to extreme events: it is due to coherent structures that tails of probability density functions become heavy, thereby increasing probabilities of extremes.[62] Meanwhile, considerable progress was made recently in transferring the extreme value theory from random phenomena to chaotic dynamical systems,[63] the Lorenz model (4) in particular.[64] As G-models beyond model (4) are also beginning to attract attention in physical and mathematical studies (e.g., Refs. 16, 45, 57, and 65–69), further progress in employing them in atmospheric studies is anticipated.

ACKNOWLEDGMENTS

This work was supported by NSF Grant AGS-1050588. We wish to thank A. Bihlo for helpful discussions.

[1]A. Pasini and V. Pelino, Phys. Lett. A **275**, 435 (2000).
[2]E. N. Lorenz, Tellus **12**, 243 (1960).
[3]E. N. Lorenz, J. Atmos. Sci. **20**, 130 (1963).
[4]A. M. Obukhov, Sov. Phys. Dokl. **14**, 32 (1969).
[5]A. M. Obukhov, Gerlands Beitr. Geophys. **82**, 282 (1973).
[6]A. Gluhovsky, Nonlinear Processes Geophys. **13**, 125 (2006).
[7]A. Gluhovsky, Sov. Phys. Dokl. **27**, 823 (1982).
[8]V. Volterra, Acta Math. **22**, 201 (1899).
[9]J. Wittenburg, *Dynamics of Multibody Systems* (Springer, 2008).
[10]A. Gluhovsky and C. Tong, Phys. Fluids **11**, 334 (1999).
[11]C. Tong, Am. J. Phys. **77**, 526 (2009).
[12]A. Gluhovsky, Izv. Acad. Sci. USSR, Atmos. Oceanic Phys. **22**, 543 (1986).
[13]A. Gluhovsky, Izv. Acad. Sci. USSR, Atmos. Oceanic Phys. **23**, 952 (1987).
[14]C. Tong and A. Gluhovsky, Phys. Rev. E **65**, 046306 (2002).
[15]V. Arnold, Ann. Inst. Fourier **16**, 319 (1966).
[16]A. Bihlo and J. Staufer, Physica D **240**, 599 (2011).
[17]A. Gluhovsky, Physica D **268**, 118 (2014).
[18]T. G. Shepherd, Adv. Geophys. **32**, 287 (1990).
[19]P. J. Morrison, Rev Mod. Phys. **70**, 467 (1998).
[20]A. Gluhovsky, C. Tong, and E. Agee, J. Atmos. Sci. **59**, 1383 (2002).
[21]A. V. Getling, *Rayleigh-Bénard Convection: Structures and Dynamics* (World Scientific Publishing Co., 1998).
[22]B. W. Atkinson and J. W. Zhang, Rev. Geophys. **34**, 403, doi:10.1029/96RG02623 (1996).
[23]V. Araújo, M. J. Pacifico, E. R. Pujals, and M. Viana, Trans. Amer. Math. Soc. **361**, 2431 (2009).
[24]M. Holland and I. Melbourne, J. Lond. Math. Soc. **76**, 345 (2007).
[25]V. Araújo and P. Varandas, Commun. Math. Phys. **311**, 215 (2012).
[26]B. Saltzman, J. Atmos. Sci. **19**, 329 (1962).
[27]Y. M. Treve and O. P. Manley, Physica D **4**, 319 (1982).
[28]J. L. Thiffeault and W. Horton, Phys. Fluids **8**, 1715 (1996).
[29]D. Roy and Z. E. Musielak, Chaos Solitons Fractals **33**, 1064 (2007).
[30]B. W. Shen, J. Atmos. Sci. **71**, 1701 (2014).
[31]D. E. Musielak, Z. E. Musielak, and K. S. Kennamer, Fractals **13**, 19 (2005).
[32]J. H. Curry, Commun. Math. Phys. **60**, 193 (1978).
[33]A. Gluhovsky, Trans. (Doklady) USSR Acad. Sci. Earth Sci. Sect. **286**, 36 (1986).
[34]Z. M. Chen and W. G. Price, Chaos Solitons Fractals **28**, 571 (2006).
[35]L. N. Howard and R. Krishnamurti, J. Fluid Mech. **170**, 385 (1986).
[36]K. B. Hermiz, P. N. Guzdar, and J. M. Finn, Phys. Rev. E **51**, 325 (1995).
[37]E. Agee and M. L. Hart, J. Atmos. Sci. **47**, 2293 (1990).
[38]A. Gluhovsky, Nonlinear Processes Geophys. **18**, 537 (2011).
[39]J. Ruppert-Felsot, O. Praud, E. Sharon, and H. L. Swinney, Phys. Rev. E **72**, 016311 (2005).
[40]A. Gluhovsky and E. Agee, J. Appl. Meteorol. Climatol. **46**, 1125 (2007).
[41]B. Efron and R. J. Tibshirani, *An Introduction to the Bootstrap* (Chapman & Hall/CRC, 1994).
[42]D. N. Politis, J. P. Romano, and M. Wolf, *Subsampling* (Springer, 1999).
[43]D. Lenschow, D. J. Mann, and L. Kristensen, J. Atmos. Oceanic Technol. **11**, 661 (1994).
[44]J. G. Charney and J. G. DeVore, J. Atmos. Sci. **36**, 1205 (1979).
[45]S. Lakshmivarahan and Y. Wang, Nonlinear Anal. RWA **9**, 1573 (2008).
[46]J. C. Robinson, ISRN Math. Anal. **2013**, 291823.
[47]L. A. Smith, Proc. Natl. Acad. Sci. U.S.A. **99**, 2487 (2002).
[48]V. Zeitlin, Physica D **49**, 353 (1991).
[49]V. Zeitlin, Phys. Rev. Lett. **93**, 264501 (2004).
[50]V. Zeitlin, Phys. Lett. A **339**, 316 (2005).
[51]A. Bihlo, Physica D **41**, 292001 (2008).
[52]P. Névir and M. Sommer, J. Atmos. Sci. **66**, 2073 (2009).
[53]R. Salazar and M. V. Kurgansky, J. Phys. A **43**, 305501 (2010).
[54]V. Lucarini, R. Blender, C. Herbert, S. Pascale, F. Ragone, and J. Wouters, Rev. Geophys. **52**, 809, doi:10.1002/2013RG000446 (2014).
[55]R. Blender and G. Badin, J. Phys. A **48**, 105501 (2015).
[56]P. Névir and R. Blender, Beitr. Phys. Atmos. **67**, 133 (1994).
[57]R. Blender and V. Lucarini, Physica D **243**, 86 (2013).
[58]J. E. Overland, D. B. Percival, and H. O. Mofjeld, Deep-Sea Res. I **53**, 582 (2006).
[59]T. P. Sapsis and A. J. Majda, Proc. Natl. Acad. Sci. U.S.A. **110**, 13705 (2013).

[60]R. J. Trapp, N. S. Diffenbaugh, and A. Gluhovsky, Geophys. Res. Lett. **36**, L01703, doi:10.1029/2008GL036203 (2009).
[61]H. W. Rust, M. Kallache, H. J. Schellnhuber, and J. Kropp, in *In Extremis*, edited by J. Kropp and H. J. Schellnhuber (Springer, 2011), pp. 61–81.
[62]J. C. McWilliams, in *Extreme Events*, edited by P. Muller, C. Garrett, and D. Henderson (University of Hawaii at Manoa, 2007), pp. 73–80.
[63]J. M. Freitas, Dyn. Syst.: Int. J. **28**, 302 (2013).
[64]A. E. Sterk, M. P. Holland, P. Rabassa, H. W. Broer, and R. Vitolo, Nonlinear Processes. Geophys. **19**, 529 (2012).
[65]S. Panchev, T. Spassova, and N. K. Vitanov, Chaos Soliton Fractals **33**, 1658 (2007).
[66]S. Lakshmivarahan and Y. Wang, J. Nonlinear Sci. **18**, 75 (2008).
[67]G. A. Leonov, Phys. Lett. A **379**, 524 (2015).
[68]M. Bianucci, J. Stat. Mech. **2015**, P05016.
[69]A. N. Souza and C. R. Doering, Physica D **308**, 26 (2015).